J Mater Sci: Mater Med (2011) 22:1993–2004
DOI 10.1007/s10856-011-4378-4

Reactive calcium-phosphate-containing poly(ester-*co*-ether) methacrylate bone adhesives: setting, degradation and drug release considerations

Xin Zhao · Irwin Olsen · Jonathan Pratten · Jonathan C. Knowles · Anne M. Young

Received: 23 November 2010 / Accepted: 9 June 2011 / Published online: 25 June 2011

Abstract This study has investigated novel bone adhesives consisting of fluid photo-polymerizable poly(lactide-*co*-propylene glycol-*co*-lactide)dimethacrylate (PGLA-DMA) mixed with systematically varying fillers of β-tricalcium phosphate (β-TCP) and monocalcium phosphate monohydrate (MCPM), for the delivery of an antibacterial drug chlorhexidine (CHX). All formulations were found to polymerize fully within 200 s after exposure to blue light. In addition, water sorption by the polymerized materials catalyzed varying filler conversion to dicalcium phosphate (DCP) (i.e. brushite and monetite). With greater DCP levels, faster degradation was observed. Moreover, increase in total filler content enhanced CHX release, associated with higher antibacterial activity. These findings thus suggest that such rapid-setting and degradable adhesives with controllable drug delivery property could have potential clinical value as bone adhesives with antibacterial activity.

X. Zhao · I. Olsen · J. C. Knowles · A. M. Young (✉)
Biomaterials and Tissue Engineering Research Department, UCL Eastman Dental Institute, 256 Gray's Inn Road, London WC1X 8LD, UK
e-mail: a.young@eastman.ucl.ac.uk

J. Pratten
Microbial Diseases Research Department, UCL Eastman Dental Institute, 256 Gray's Inn Road, London WC1X 8LD, UK

J. C. Knowles
WCU Research Centre of Nanobiomedical Science, Dankook University, San#29, Anseo-dong, Dongnam-gu, Cheonan-si, Chungnam 330-714, South Korea

1 Introduction

With increased life expectancy, there is a growing need for minimally invasive techniques to replace or repair damaged or diseased bone. Injectable degradable adhesives such as poly(lactide-*co*-propylene glycol-*co*-lactide)dimethacrylates (PGLA-DMA) have therefore been developed for this purpose, i.e., to fill in the bone defects of different shape, provide structural support and enhance bone repair [1]. Compared with conventional non-degradable methacrylate bone adhesives, the PGLA-DMA adhesives can be solidified within seconds of blue light exposure, with low shrinkage and heat generation during cure [1]. In addition, the set PGLA-DMA adhesives have readily controllable mechanical and degradation properties [1, 2] and, importantly, they have been shown to be biocompatible with bone cells [3].

Reactive calcium phosphate particles of β-tricalcium phosphate (β-TCP) and monocalcium phosphate monohydrate (MCPM) (powder components of brushite—forming bone cements [4]) have previously been added as fillers to PGLA-DMA adhesives to further reduce heat generation and shrinkage during adhesive polymerization [2, 3]. Additionally, upon incorporation of β-TCP and MCPM particles, hydrolytic degradation of such polymers is often increased, with concomitant neutralization of acidic degradation products [2, 3]. The fillers of β-TCP and MCPM have also been found to react and precipitate as dicalcium phosphate (DCP) (i.e. brushite and monetite) upon water sorption, increasing calcium phosphate particle dispersion and material modulus [2]. Moreover, the subsequent slow DCP dissolution then generates calcium and phosphate ions that may aid bone re-mineralization [3]. Furthermore, after implantation into chick embryo femurs, the composite adhesives have been shown to be in close contact with the

adjacent bone, with no indication of adverse immunological reaction [3].

Nevertheless, the service life of such medical implants can be reduced as a result of bacterial infections, which may prevent effective wound healing processes taking place [5]. Thus, controlled release of an antibacterial would be of substantial clinical value in limiting bacteria infection [6]. As previously reported, the bacterium *Staphylococcus aureus* (*S. aureus)* is often commonly associated with bone infections [7, 8] and is also generally highly susceptible to the antibacterial agent chlorhexidine (CHX) [9]. This drug has been found to have very low incidence of resistance development [10] and minimal toxicity to host cells [11–14]. In this study, adhesives were therefore prepared consisting of fluid PGLA-DMA containing β-TCP and MCPM as fillers, with CHX added as an antibacterial drug. The effects of addition of filler and CHX were measured on several material properties, including polymerization rate and degree of monomer conversion, water sorption and material degradation, water accelerated chemistry changes, CHX release kinetics and antibacterial activity.

2 Materials and methods

2.1 Materials

Triethylamine (98%), methacryloyl chloride (97%) and β-TCP (95%), were purchased from Fluka, Gillingham, UK. D,L-Lactide was obtained from Purac, Gorinchem, The Netherlands. Poly(propylene glycol) (average molecular weight = 1000 g/mol), camphorquinone (CQ, 97%), *N*,*N*-dimethyl-*p*-toluidine (DMPT, 99%), 2-hydroxyethyl methacrylate (HEMA, 99%), chlorhexidine diacetate (98%), MCPM (99%) were purchased from Sigma–Aldrich, Gillingham, UK. MCPM particles were sieved to obtain two different size ranges of 20–38 and 75–106 μm (denoted as 30 and 90, respectively).

2.2 Monomer synthesis

The PGLA-DMA adhesive (denoted $P_{17}L_4$ in earlier work [1]) was synthesized using the following procedure. Poly(propylene glycol) (0.1 mol) containing 0.05 wt% stannous octoate was reacted under nitrogen with lactide (0.4 mol) for 6 h at 150°C. After addition of dichloromethane and cooling in an ice bath, 0.4 mol triethylamine and 0.4 mol methacryloyl chloride were slowly added. Subsequent addition of acetone promoted precipitation of triethylamine·HCl. After removal of the bulk of this by-product by filtration, the filtrate was repeatedly washed with aqueous HCl followed by $NaHCO_3$ solution (0.1 M of either) and finally water. The resultant hydrophobic dichloromethane phase was separated from the aqueous phases and the final product obtained by rotary evaporation to remove the residual solvent.

The product was expected to be a triblock oligomer (short polymer) capped at each end with a methacrylate group. Its total molecular weight was expected to be 1712 g/mol and consist of 17 propylene glycol units ($(CH_2CH(CH_3)O)_{17}$) with on average of two lactide molecules (i.e.$(C(CH_3)COO)_4$) attached to each end. The molecular structure and purity of the synthesized monomer was confirmed using nuclear magnetic resonance (NMR) spectroscopy (600 MHz Varian Unity INOVA Spectrometer, Palo Alto, CA, USA) as previously reported [1].

2.3 Sample preparation

PGLA-DMA (90 wt%) was mixed with CQ (1 wt%), DMPT (1 wt%) and HEMA (8 wt%) to produce the organic phase. This was then added with 50 wt% or 70 wt% filler (F%). The filler consisted of β-TCP (T) and MCPM (M), with T/M = 1 or 4 (mol/mol). The median diameter of the MCPM particle (M_d) was 30 or 90 μm. With three variables (F%, T/M and M_d), each at two levels, there are eight possible formulations (see Table 1 for details). CHX (10 wt% of the total mixture) was then added to each formulation. Polymer and composites without CHX were used as controls to assess the effect of CHX addition on material properties including polymerization, water-induced mass, volume and chemical changes. Polymer discs with CHX were additionally used as control to investigate the effect of filler addition on CHX release rate and antibacterial activity in addition to the above-mentioned material properties.

Polymerized discs of 5 (for agar diffusion tests) or 12 mm diameter (for all other studies) and 2 mm thickness were obtained by placing the composite pastes into steel rings. The top and bottom surfaces were covered by acetate sheets (AF 4301, 3M, Manchester, UK) and the samples cured in a light box (Triad® 2000™ visible light cure system, Dentsply Trubyte, Palo Alto, CA, USA) using blue light (100 mW/cm^2) for 12 min. Raman spectroscopy was then used to confirm full polymerization (i.e. no detectable peak at 1640 cm^{-1} due to 'C=C' of PGLA-DMA). Each test was performed in triplicate, and results are expressed as means ± standard deviation (SD).

2.4 Polymerization kinetics

To quantify polymerization kinetics, unset material formulations were placed on a Golden Gate™ heated diamond ATR top-plate at 37°C, within a Fourier transform infrared (FTIR) spectrometer (Perkin-Elmer, Series 2000, Beaconsfield, UK). The paste was confined within a ring

Table 1 Polymerization rate, initial mass and volume change, final water content and material loss of composites and polymer

	Formulations	F% (%)	T/M	M_d (μm)	Polymerization rate (%/s)		Initial mass change (%)		Initial volume change (%)		Final water content (%)		Final material loss (%)	
					− CHX	+ CHX	− CHX	+ CHX	− CHX	+ CHX	− CHX	+ CHX	− CHX	+ CHX
Composites	1	70	4	90	0.9 ± 0.2	0.9 ± 0.2	12 ± 1	13 ± 1*	20 ± 1	24 ± 1*	11 ± 1	20 ± 1*	4 ± 1	4 ± 1
	2	70	4	30	1.0 ± 0.2	0.9 ± 0.2	11 ± 1	12 ± 1*	20 ± 1	22 ± 1*	11 ± 1	19 ± 1*	4 ± 1	4 ± 1
	3	70	1	90	0.9 ± 0.2	1.0 ± 0.2	18 ± 1	20 ± 1*	32 ± 1	39 ± 1*	20 ± 1	40 ± 2*	10 ± 1	10 ± 1
	4	70	1	30	0.9 ± 0.2	0.9 ± 0.2	19 ± 1	21 ± 1*	32 ± 1	37 ± 1*	21 ± 1	33 ± 2*	10 ± 1	9 ± 1
	5	50	4	90	1.7 ± 0.3	1.6 ± 0.3	6 ± 1	8 ± 1*	8 ± 1	14 ± 1*	8 ± 1	15 ± 1*	4 ± 1	4 ± 1
	6	50	4	30	1.6 ± 0.3	1.5 ± 0.3	6 ± 1	7 ± 1*	10 ± 1	11 ± 1*	9 ± 1	12 ± 1*	4 ± 1	4 ± 1
	7	50	1	90	1.6 ± 0.3	1.6 ± 0.3	8 ± 1	12 ± 1*	15 ± 2	18 ± 1*	14 ± 1	23 ± 1*	8 ± 1	10 ± 1
	8	50	1	30	1.7 ± 0.3	1.6 ± 0.3	10 ± 1	10 ± 1	13 ± 1	14 ± 1	15 ± 1	20 ± 2*	9 ± 1	10 ± 1
Polymer					1.6 ± 0.3	1.6 ± 0.3	2 ± 1	5 ± 1*	2 ± 1	5 ± 1*	4 ± 1	8 ± 1*	3 ± 1	4 ± 1

F% (total filler content), T/M (molar ratio of β-TCP to MCPM) and M_d (MCPM particle size) are three variables involved in the composite filler factorial design. Polymerization rate was defined as the gradient of the plot of 'monomer conversion percentage versus light exposure time (between 20 and 60% conversion)'. Initial mass change was determined as the mass change after 24 h of water immersion relative to the original mass of the specimen, defined as 100% (see Eq. 1). Initial volume change was determined as the volume change after 24 h of water immersion relative to the original volume of the specimen, defined as 100% (see Eq. 4). Final water content was calculated as the percentage (by weight) of the water present in the wet specimens relative to the wet specimens after 10 weeks of water immersion (see Eq. 5). Final material loss was calculated as the percentage of the mass of eroded material after 10 weeks of water immersion relative to the original dry mass (without the drug) prior to water immersion (see Eq. 6). '−' and '+' stand for formulations without and with CHX, respectively. Results = means ± SD ($n = 3$)

* Significant differences ($P < 0.05$) from control values (formulations without CHX)

of 5 mm diameter and 2 mm depth. The top surface of the paste was sealed with an acetate sheet. FTIR spectra of the lower few microns of the sample in contact with the diamond were then generated every 8 s for 30 min using Timebase software. The wavenumber range was 500–4000 cm^{-1} and resolution 4 cm^{-1}. Each mixture was exposed to blue light (400 mW/cm^2) using a Coltolus dental light curing gun (Coltene®, Burgess Hill, UK) for 120 s.

The rationale behind the following method of data analysis has been described previously [1]. Briefly, the difference in FTIR absorbance at 1716 and 1736 cm^{-1} was recorded and the change between time t = 0 and t calculated. This was divided by the maximum change between the beginning and end of the experiment to calculate the extent of the reaction. Multiplication by the final percentage reaction (i.e. degree of monomer conversion, see below) then gave monomer reacted versus time. Polymerization rate, gradient of the plot of 'monomer conversion percentage versus light exposure time (between 20 and 60% conversion)', was subsequently calculated and reported.

Final percentage reacted can usually be obtained more accurately from Raman than from FTIR due to the very strong intensity of the Raman 'C=C' stretch peak. The average Raman spectra of samples before and after polymerization were therefore obtained using a LabRam spectrometer (Horiba Jobin–Yvon, Stanmore, UK). This instrument was equipped with a 633 nm wavelength laser, ×50 objective lens and 1800 grating. All spectra were background subtracted and normalized by the 'C–H' peak at 1447 cm^{-1}. The height of the Raman 'C=C' peak at 1640 cm^{-1} after light cure divided by that of the uncured pastes was used to gain the final fraction of monomer remaining. This was then converted to final percentage reacted [1].

2.5 Mass and volume change upon water sorption

Mass and density of the set specimen discs (12 mm diameter, 2 mm thick) were assessed using an electronic balance with a density kit (Mettler Teledo, Osaka, Japan). The measured densities of the initial dry specimens were also used to confirm negligible air incorporation (i.e. the practical density was identical to the calculated theoretical density within experimental error). The discs were subsequently placed upright in the conical end of a Sterilin tube, containing 10 ml of neutral de-ionized water (pH 7, adjusted using 0.01 mol/l NaOH). After 15 min, 2, 8, 24 h, 2, 7 and 10 days and 3, 5, 6, 7, 8, 9 and 10 weeks at 37°C, the mass and density were again measured prior to placement of samples in fresh storage solution. Percentage wet mass (ΔM_t) change due to combined water sorption, material loss and drug release was calculated using:

$$\Delta M_t = \frac{M_t - M_0}{M_0} \times 100 \quad (1)$$

where M_t and M_0 are the wet mass of the specimen at time t and initial dry mass, respectively (both measured in air).

In order to determine sample volume change, sample density at time t was first measured using:

$$\rho_t = \rho_{water} \times \frac{M_t}{M_t - M_{t,w}} \quad (2)$$

where ρ_t is the wet density of the specimen at time t and ρ_{water} is the density of water at the operating temperature; M_t and $M_{t,w}$ are the mass of the wet specimen measured in air and in water at time t.

Volume change (ΔV_t) was then determined using:

$$V_t = \frac{M_t}{\rho_t} \quad (3)$$

$$\Delta V_t = \frac{V_t - V_0}{V_0} \times 100 \quad (4)$$

where V_t and V_0 are the wet volume of the specimen at time t and initial dry volume, respectively.

At the end of the study period, specimens were dried under vacuum to constant mass. The final water content (W_c) and material loss (M_l) was calculated using:

$$W_c = \frac{M_f - M_{f,d}}{M_f} \times 100 \quad (5)$$

$$M_l = \frac{M_0 - M_f - M_d}{(1 - y)M_0} \times 100 \quad (6)$$

where M_f, $M_{f,d}$ and M_d are respectively the final wet and dry mass and mass of the released drug. y is the initial mass fraction of CHX (i.e. 10 wt%).

2.6 Water accelerated chemical changes

Samples stored as above for 24 h and 10 weeks in water were additionally analyzed using Raman and XRD. Each specimen was cut vertically (for Raman) and horizontally (for XRD) with a razor blade to expose their centre for analysis. To generate Raman "line" spectra, 31 "point" spectra were obtained every 5 μm along a 150 μm line drawn parallel to the top surface of the specimen. These line spectra were recorded every 100 μm from the top surface to the center of the specimen. Background subtraction was performed using Labspec software for each single point spectrum. Mean sample spectra were then generated by averaging the 10 line spectra. The mean spectra were normalized using the polymer 'C–H' peak at 1447 cm^{-1}. The peak intensities due to other components then provide a semi-quantitative indication of the level of that component relative to the polymer [2, 15].

In the following the spectra of formulations with CHX were provided. Corresponding spectra of formulations without drug were as previously reported [3]. Peaks were assigned to polymer, β-TCP, MCPM, brushite (hydrous DCP), monetite (anhydrous DCP) and CHX by using the spectra of the pure components.

Although Raman can readily detect β-TCP and MCPM, it is less sensitive for distinguishing brushite and monetite due to their overlapping spectra (see Sect. 3). The presence of brushite and monetite, however, can be readily identified using XRD. XRD spectra were obtained using a Brüker D8 advance diffractometer (Karlsruhe, Germany), with Ni filtered Cu Kα radiation. Data were collected from 10° to 100° 2θ with a step size of 0.02° in a count time of 18.9 s using a Bruker Lynx Eye detector. In addition to the International Centre for Diffraction Data database volumes 1, spectra of pure components were used to assign peaks of different calcium phosphates [16].

2.7 In vitro CHX release

To quantify the rate of CHX release, UV absorbance spectra of the above sample storage solutions were measured between 200 and 350 nm using a Unicam UV 500 Thermospectronic® Spectrometer (Thermo Spectronic, Cambridge, UK). These were compared with solution spectra of pure CHX at concentrations of 5–50 μg/ml. The CHX concentration was converted to cumulative mass of CHX released into the storage solution and then to the percentage of the released CHX relative to the total CHX in the original sample [6, 15].

2.8 Antibacterial susceptibility assessment

The antibacterial activity of the polymer and composites containing CHX was assessed by an agar diffusion assay (British Society for Antimicrobial Chemotherapy standardized disc susceptibility testing method [17]), using bacterial strains of *S. aureus* 8325-4 (SA 8325-4) and methicillin-resistant *S. aureus*-16 (MRSA-16). Briefly, an overnight culture of known OD of the test bacterium was spread onto the surface of isosensitest agar plates (Oxoid, Basingstoke, UK) before sample discs (5 mm diameter, 2 mm thick) were placed on top. The plates were incubated at 37°C in a 5% CO_2 atmosphere for 24 h. Diameters of inhibition zones (including specimens) were measured in three different directions using calipers.

2.9 Statistics

The statistical significance of differences between the materials with and without CHX on various material properties including polymerization rate, initial mass and volume change, final water content and material loss, was evaluated using one-way ANOVA with the Bonferroni post hoc test. Data were evaluated using SPSS 14.0 for Windows (SPSS, Inc., Chicago, Ill., USA). The results were expressed as means ± SD, and P values <0.05 were considered statistically significant.

2.10 Factorial analysis

Factorial analysis was used in this study to assess the effect of three variables (F%, T/M and M_d) on different material properties (P in Eq. 7) of formulations containing CHX [1, 3, 6, 15]. These material properties included polymerization rate, initial mass and volume change, final water content, final material mass, CHX release at 10 days and 10 weeks, and antibacterial activity.

$$\ln P = \langle \ln P \rangle \pm a_{F\%} \pm a_{T/M} \pm a_{M_d} \quad (7)$$

where $\langle \ln P \rangle$ is the average value of ln P for all 8 possible formulations (see details in Table 1). $a_{F\%}$, $a_{T/M}$ and a_{M_d} quantify the average effect of raising F%, T/M and M_d, respectively from their low to high values on each material property. Values of 'a' were determined in triplicate using a method previously described [1, 3, 6, 15] and expressed as means ± SD. If 'a value (means ± SD)' does not cross zero, the variable has on average a significant effect on the particular property. A positive 'a value' means that the property increases with increasing variable and vice versa for a negative 'a'. Higher values of 'a' indicate greater effects of the variable on the property.

3 Results

3.1 Synthesized monomer structure

NMR confirmed that the level of lactide and subsequent methacrylate attachment to poly(propylene glycol) were 97 and 95%, respectively, of the values expected. Thus, the monomer structure was as predicted, a triblock oligomer consisting of 17 propylene glycol units, 4 lactide molecules and 2 methacrylate groups.

3.2 Effect of CHX and filler addition on polymerization rate and degree of monomer conversion

Polymerization on the FTIR diamond began immediately upon turning on the high intensity curing light irrespective of formulations (see example in Fig. 1). For formulations with the same level of filler (see example in Fig. 1, circle or square), the curves of monomer conversion percentage versus light exposure time of formulations with CHX

(filled symbols) overlapped with those without CHX (non-filled symbols). There was no significant difference in the polymerization rate between the samples with and without CHX (Table 1), demonstrating that the CHX concentration had no apparent effect on the polymerization rate.

Additionally, increasing the filler content from 50 to 70 wt% resulted in slower polymerization (see example in Fig. 1, compare circle and square) although adding filler to the polymer at a level of 50 wt% had no measurable effect. The average polymerization rate was found to be ~1.7%/s for polymer and composites with F% = 50% (C_{F50}, i.e., formulations 5–8 in Table 1) and ~0.9%/s for C_{F70} (i.e., formulations 1–4 in Table 1). According to factorial analysis, the only variable which significantly affected the polymerization rate was the total filler content, F% (Table 2).

For all samples, over 85% of the monomer was polymerized following 120 s of blue light exposure and 100% monomer conversion was observed by 200 s (see example in Fig. 1). This result established that the final degree of monomer conversion was not affected by CHX and filler addition.

3.3 Effect of CHX and filler addition on water induced mass and volume change

Polymer exhibited small and comparable mass (5 ± 1%) and volume (5 ± 1%) increase during the initial 24 h of water immersion (Table 1). All composite discs increased rapidly in mass (Fig. 2a) during the initial 24 h of water submersion, but more so in volume (Fig. 2b). Formulations with F% = 50% and T/M = 4 (i.e., formulations 5 and 6 in Table 1) exhibited minimum mass (approximately 8%) and volume (approximately 13%) change whereas those with F% = 70% and T/M = 1 (i.e., formulations 3 and 4 in Table 1) showed the maximum mass (approximately 21%) and volume (approximately 38%) increase (Table 1). Control samples without CHX showed similar trend in the initial mass and volume change but these changes were smaller compared to the formulations with CHX ($P < 0.05$, Table 1). This result demonstrated that addition of CHX significantly raised the initial mass and volume change of polymer and composites.

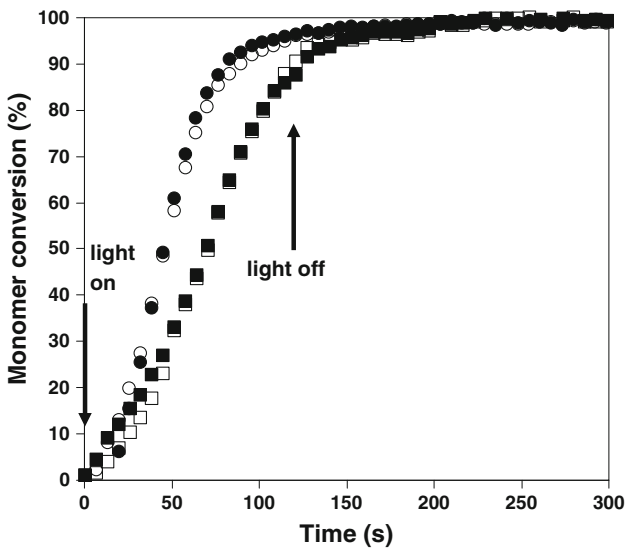

Fig. 1 Photo-polymerization of representative composite formulations. The results demonstrate the lack of effect of drug but decline in rate with higher filler content. (*Filled square* and *open square*) F% = 70%, T/M = 4, M_d = 30 μm with and without CHX, respectively; (*filled circle* and *open circle*) F% = 50%, T/M = 4, M_d = 30 μm with and without CHX, respectively

Factorial analysis showed that initial mass and volume change was affected strongly by F% and T/M, but less so by M_d (Table 2). Increase in F% and decrease in T/M (i.e. increase in MCPM content of the specimens), encouraged greater water sorption and thus mass and volume increase. Composites with large M_d also exhibited higher mass and volume change compared to those with small M_d. The water dominated early mass increase was also confirmed by the result that the initial volume change divided by mass was comparable with the initial sample densities (data not shown). The water content increased linearly with the proportion of the MCPM in the composites: increase in 1 g of MCPM would lead to increase in 0.46 g of water sorption (data not shown).

Between 24 h and 10 weeks, a slight decrease in polymer and composite mass and a less reduction in volume (compared to mass decrease) were generally observed (Fig. 3, compare a and b), indicative of a combined bulk and surface erosion during the hydrolytic degradation. Addition of CHX had no measurable effect on the final material loss of either the polymer or the composites although the drug addition significantly raised the final water content ($P < 0.05$, Table 1).

Furthermore, factorial analysis established that varying the F% or the M_d, had no substantial effect on the final mass loss (Table 2). However, decrease in T/M significantly enhanced final material loss. Composites with T/M = 1 ($C_{T/M1}$, i.e., formulations 3, 4, 7 and 8 in Table 1) exhibited maximum final mass loss (~10%) whereas $C_{T/M4}$ (i.e., formulations 1, 2, 5 and 6 in Table 1) exhibited lower material loss than $C_{T/M1}$ but comparable mass loss to the polymer (~4%) (Table 1).

3.4 Effect of CHX and filler addition on water accelerated chemical changes

3.4.1 Raman

In general, no characteristic 'C=C' peak at 1640 cm^{-1} was observed in any of the polymer and composite Raman

Table 2 Effect of filler addition on different material properties

	Polymerization rate	Initial mass change	Initial volume change	Final water content	Final material loss	CHX release at 10 days	CHX release at 10 weeks	Inhibition zone sizes	
								SA 8325-4	MRSA-16
F%	-0.6 ± 0.02	0.6 ± 0.1	0.7 ± 0.1	0.5 ± 0.1	–	0.7 ± 0.01	0.9 ± 0.01	0.5 ± 0.04	0.5 ± 0.1
T/M	–	-0.4 ± 0.02	-0.4 ± 0.02	-0.6 ± 0.1	-0.8 ± 0.1	–	–	–	–
M_d	–	0.1 ± 0.02	0.1 ± 0.04	0.1 ± 0.08	–	–	–	–	–

F% (total filler content), T/M (molar ratio of β-TCP to MCPM) and M_d (MCPM particle size) are three variables involved in the filler factorial design. The results shown are 'a values' calculated using Eq. 7. Results = means ± SD ($n = 3$). The magnitude of the 'a' value and its sign indicate the size and direction of the effect of each variable on a material property. '−' means that the effect of a variable on a property is negligible

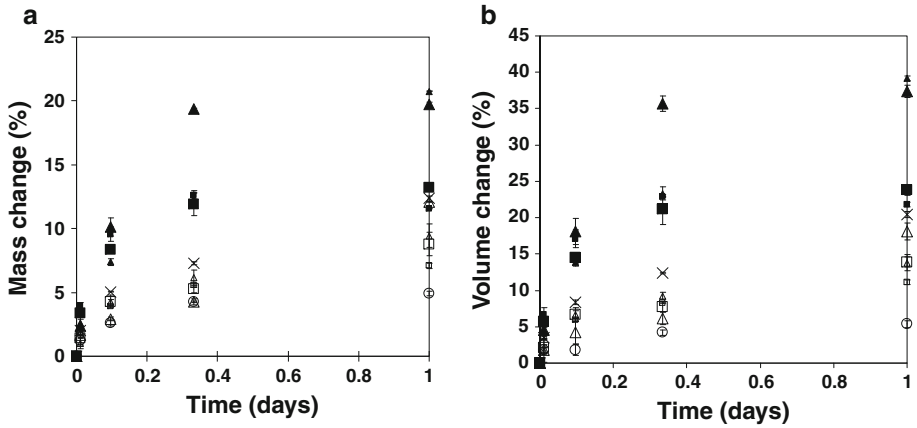

Fig. 2 Initial mass (**a**) and volume (**b**) change of polymer and composites after water immersion. (*Open circle*) polymer; (*open square* and *small open square*) F% = 50%, T/M = 4, M_d = 90 and 30 μm, respectively; (*open triangle* and *small open triangle*) F% = 50%, T/M = 1, M_d = 90 and 30 μm; (*filled square* and *small filled square*) F% = 70%, T/M = 4, M_d = 90 and 30 μm; (*filled triangle* and *small filled triangle*) F% = 70%, T/M = 1, M_d = 90 and 30 μm

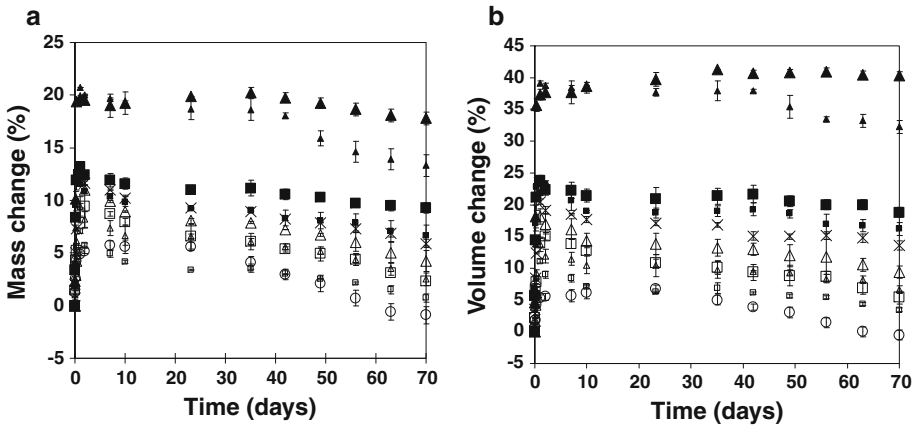

Fig. 3 Mass and volume change of polymer and composites after water immersion. (*Open circle*) polymer; (*open square* and *small open square*) F% = 50%, T/M = 4, M_d = 90 and 30 μm, respectively; (*open triangle* and *small open triangle*) F% = 50%, T/M = 1, M_d = 90 and 30 μm; (*filled square* and *small filled square*) F% = 70%, T/M = 4, M_d = 90 and 30 μm; (*filled triangle* and *small filled triangle*) F% = 70%, T/M = 1, M_d = 90 and 30 μm

spectra, consistent with full monomer conversion after light exposure. By comparison with the standard CHX compound, no shift of characteristic CHX peaks were observed before and after photo-polymerization and upon 24-h or 10-week storage in water, indicative of maintenance of CHX chemical structure after light exposure and water storage.

The major factors affecting the chemical components of the set composites after immersion in water were CHX and T/M, as shown in Raman and XRD spectra. In the Raman spectra, with T/M = 1, β-TCP (main peaks at 945 and 970 cm^{-1}), MCPM (main peaks at 903 and 915 cm^{-1}) and CHX (main peaks at 1093, 1298 and 1600 cm^{-1}) were initially readily detectable (see example in Fig. 4a). After

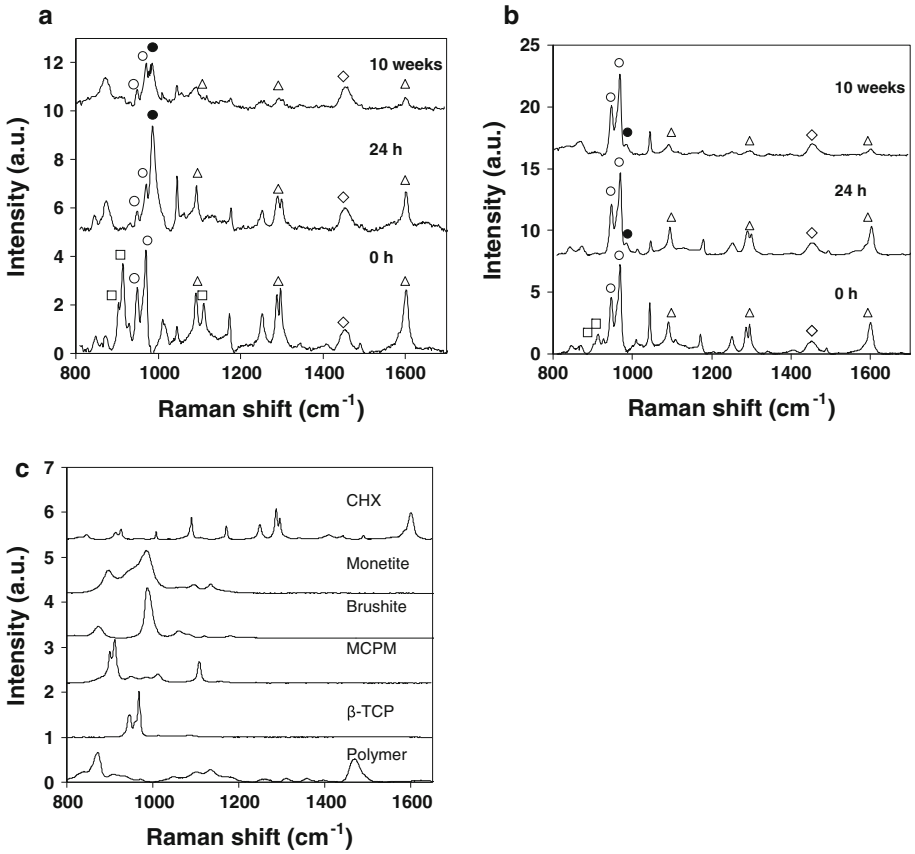

Fig. 4 Raman spectra of representative composite formulations containing CHX. **a** F% = 70%, T/M = 1 and M_d = 30 μm and **b** F% = 70%, T/M = 4 and M_d = 30 μm before (0 h) and after 24 h and 10 weeks of immersion in water. (*Open diamond*) polymer; (*open circle*) β-TCP; (*open square*) MCPM; (*filled circle*) dicalcium phosphate, i.e., brushite and monetite; (*open triangle*) CHX. **c** Raman spectra of standards including the set polymer, β-TCP, MCPM, brushite, monetite and CHX

24 h of water immersion, the MCPM peaks were no longer detected. Those of β-TCP and CHX were also substantially reduced, and a peak at 980 cm^{-1}, assigned to DCP, i.e., brushite and monetite, appeared. The brushite peak was more intense for those formulations containing CHX. In the absence of CHX, spectra were consistent with greater monetite formation. After 10 week of water immersion, the brushite and CHX peaks declined but the β-TCP peaks remained (see example in Fig. 4a).

Conversely, with T/M = 4, the β-TCP peaks dominated the Raman spectra and changed very little in intensity with time (see example in Fig. 4b). The small MCPM peaks and the presence of DCP were barely detectable in the 24-h and 10-week Raman spectra. Although CHX was readily detectable in the 0 and 24-h specimens, the CHX peaks were less intense in the 10-week Raman spectra.

3.4.2 XRD

In the XRD spectra, with T/M = 1, β-TCP (main peaks at 27.9°, 31.2° and 34.5° 2θ) and MCPM (main peaks at 23° and 24.3° 2θ) were clearly observed prior to water immersion (see example in Fig. 5a). After 24 h, the β-TCP peaks became less pronounced and the MCPM peaks were not detected. However, intense peaks at 12°, 21° and 29.4° 2θ (assigned to brushite) and at 26.7° and 30.3° 2θ (assigned to monetite), became apparent. The ratio of peak intensity of brushite to monetite was higher in the presence of CHX compared to that of the formulations without CHX. After 10 weeks of water immersion, only monetite and β-TCP peaks were detected.

Conversely, with T/M = 4, the β-TCP peaks dominated the composite XRD spectra at all times including 0 h, 24 h and 10 weeks (see example in Fig. 5b). MCPM, brushite and monetite were all detectable but at much lower intensity. MCPM was observed in the 0-h specimen spectra and brushite was detected in the 24-h specimen spectra. Monetite was seen in both the 24-h and 10-week spectra but with reduced intensity after specimen immersion in water for 10 weeks. CHX could not be detected in any XRD spectra.

The above results were consistent with the formation of brushite and monetite in 24 h as a result of the reaction of β-TCP and MCPM. It was also found that the CHX addition raised the formation of brushite over monetite when composites had T/M = 1. In the formulations with T/M = 4, the effect of CHX addition was less pronounced. During long-term water immersion, any produced brushite and monetite has largely dissolved into the storage solution.

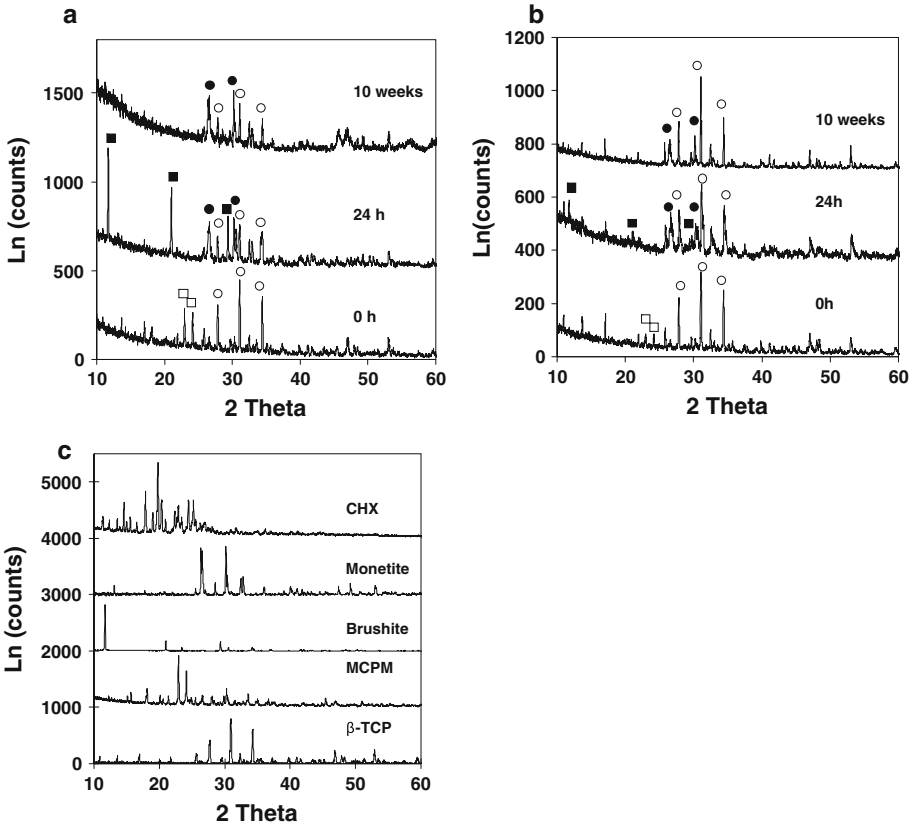

Fig. 5 XRD spectra of representative composite formulations containing CHX. **a** F% = 70%, T/M = 1 and M_d = 30 μm and **b** F% = 70%, T/M = 4 and M_d = 30 μm before (0 h) and after 24 h and 10 weeks of immersion in water. (*Open circle*) β-TCP; (*open square*) MCPM; (*filled square*) brushite; (*filled circle*) monetite. CHX could not be detected in any XRD spectra. **c** XRD spectra of standards including β-TCP, MCPM, brushite, monetite and CHX

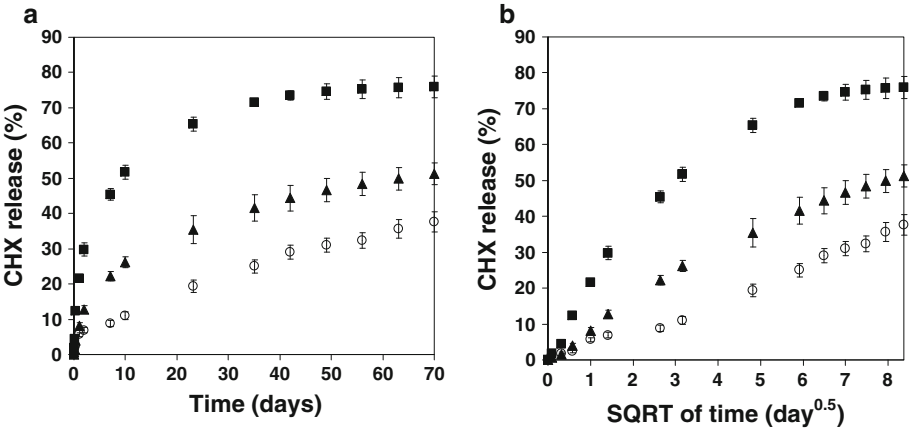

Fig. 6 CHX release from the set polymer and composites. The percentage of the released CHX relative to the total CHX in the original sample is plotted versus time (**a**) and square root (SQRT) of time (**b**). (*Open circle*) polymer; (*filled triangle*) composites with F% = 50%; (*filled square*) composites with F% = 70%

3.5 Effect of filler addition on CHX release

UV spectra of sample storage solutions exhibited identical profiles to those of pure CHX solutions, demonstrating that the CHX was released without damage in chemical structure (data not shown). CHX was released faster in the initial 10 days and then the release rate declined with time. CHX release rate increased in the order: polymer < C_{F50} < C_{F70} (see example in Fig. 6a). At 10 days, the cumulative CHX release was 11, 26 and 52% of the original CHX when the filler content increased from 0, 50 to 70 wt%, respectively. At 10 weeks, the cumulative CHX release from polymer, C_{F50} and C_{F70} was 37, 57 and 77%, respectively (Table 3). Factorial analysis showed that F% was the only factor having a significant effect on CHX release kinetics, with CHX release enhanced by raising F% (Table 2).

The plot of CHX release versus square root of time was more linear than that versus time (compare Fig. 6a and b), as expected for a diffusion-controlled process. The gradients of the curves (CHX release percentage versus square root of time) representing polymer and C_{F50} were almost constant at any time points whereas the gradients of the curves of C_{F70} kept constant in the initial 10 days but decreased at a high release percentage of 60%.

Table 3 Cumulative CHX release at 10 days and 10 weeks; bacterial inhibition zone sizes of composites and polymer

	Formulations	F% (%)	T/M	M_d (μm)	CHX release at 10 days (%)	CHX release at 10 weeks (%)	Inhibition zone diameter (mm)	
							SA 8325-4	MRSA-16
Composites	1	70	4	90	54 ± 1	75 ± 1	14 ± 1	13 ± 1
	2	70	4	30	50 ± 5	80 ± 5	14 ± 1	13 ± 1
	3	70	1	90	53 ± 2	74 ± 1	13 ± 1	11 ± 1
	4	70	1	30	50 ± 5	77 ± 5	15 ± 1	13 ± 1
	5	50	4	90	27 ± 1	59 ± 2	12 ± 1	11 ± 1
	6	50	4	30	24 ± 1	58 ± 1	12 ± 1	11 ± 1
	7	50	1	90	28 ± 1	58 ± 1	12 ± 1	11 ± 1
	8	50	1	30	26 ± 3	54 ± 1	12 ± 1	10 ± 1
Polymer					11 ± 1	37 ± 3	11 ± 1	10 ± 1

F% (total filler content), T/M (molar ratio of β-TCP to MCPM) and M_d (MCPM particle size) are three variables involved in filler factorial design. Results = means ± SD ($n = 3$). SA 8325-4 and MRSA-16 are bacterial strains of *S. aureus*

3.6 Effect of CHX and filler addition on adhesive antibacterial activity

Although a small thin halo of growth inhibition around some of the control formulations with no CHX was occasionally observed, all the CHX-containing formulations (both polymer and composites) had very much larger and clearer inhibition zones. The sizes of these increased as the F% increased, with diameters for the *S. aureus* of 11, 12 and 14 mm for 0, 50 and 70 wt% filler, respectively. With the MRSA, the zone diameters were very similar, with an average of 10, 11 and 13 mm for 0, 50 and 70 wt% filler, respectively (Table 3).

Factorial analysis showed that F% was the only factor having a significant effect on the sizes of the inhibition zones, with zone diameters enlarged by raising the F% (Table 2).

4 Discussion

In this paper, several material properties including polymerization rate and degree of monomer conversion, water sorption and material degradation, water accelerated chemistry changes, CHX release kinetics and adhesive antibacterial activity were investigated and the effect of CHX and filler addition on these properties analyzed.

4.1 Effect of CHX and filler addition on polymerization rate and degree of monomer conversion

The lack of effect of CHX addition on the monomer polymerization rate found here is similar to a previous study of photo-polymerization kinetics of non-degradable methacrylate composites [15]. Although in that study CHX had been found to increase the subsequent dark cure, the enhanced dark cure effect was not detected in the present study possibly because the monomer conversion percentage was already more than 85% when the light was turned off. However, a high level of filler addition (i.e. 70 wt%) was found to reduce the polymerization rate, which may have been due to the increased scattering of the initiating blue light because of the high level of filler particles.

All formulations were found to set rapidly and completely on light exposure, with full monomer conversion achieved regardless of CHX and filler addition. Such fast and full cure as shown here could allow rapid material bonding to surrounding tissues after injection and would, additionally, limit the release of reactive and potentially toxic double bond-containing monomers (PGLA-DMA) in vivo [1].

4.2 Effect of CHX and filler addition on water sorption and hydrolytic degradation

The initial increase in mass and volume could be ascribed to water sorption, which exceeded material degradation and drug release. The addition of CHX raised the early water sorption of both the polymer and composites, possibly because the water-soluble nature of CHX would increase internal osmotic pressure and enhance water sorption [6]. Increase in the amount of MCPM present per specimen was found to substantially enhance early water sorption. Thus, with molar ratios of β-TCP ($Ca_3(PO_4)_2$)/MCPM ($Ca(H_2PO4)_2{\cdot}H_2O$) of 4 or 1, the amount of MCPM was found to determine the water needed for brushite ($CaHPO_4{\cdot}2H_2O$) formation, according to the following equation, with 0.5 g of water being required to convert 1 g of MCPM into brushite [4]:

$$Ca_3(PO_4)_2 + Ca(H_2PO_4)_2{\cdot}H_2O + 7H_2O \rightarrow 4CaHPO_4 \cdot 2H_2O$$

The water sorption levels found in this paper were just sufficient for this reaction to occur. This may explain the

formation of monetite (Ca $(H_2PO4)_2$) in addition to brushite, as shown by the Raman and XRD analysis (see below).

Larger MCPM particles were also found to enhance early water sorption. MCPM with large particle sizes would be expected to dissolve and react more slowly, thereby increasing the time over which MCPM was present in the formulations and thus enhancing the early water sorption. In addition, CHX was also found to raise the material final water content, possibly due to the replacement of released CHX with water, increasing the water percentage. However, the final material loss was not affected by CHX concentration. Moreover, based on factorial analysis, final material loss was enhanced by reducing T/M. This may be associated with the different chemical compositions (e.g., β-TCP or DCP) of the composites after immersion in water due to different T/M as shown in Raman and XRD studies (see below).

4.3 Effect of CHX and filler addition on water accelerated chemical changes

Raman and XRD results were consistent with the reaction of β-TCP and MCPM to form brushite and monetite upon water sorption in 24 h in absence or presence of CHX, irrespective of composite formulations. Higher ratios of brushite over monetite of the formulations containing CHX than those without CHX were observed in 24 h Raman and XRD spectra [3]. This might be due to the basic nature of CHX which may help stabilize brushite and prevent its conversion to monetite in the presence of water [18]. Additionally, as shown in this study, CHX addition raised the initial water sorption which may promote more brushite (hydrous DCP) formation.

The major factor affecting the composite chemical composition after immersion in water was T/M. With T/M = 1, brushite and monetite were the major calcium phosphates after placement in water whereas with T/M = 4, β-TCP was the major calcium phosphate. $C_{T/M1}$ would thus degrade faster than $C_{T/M4}$ as brushite and monetite have higher solubility than β-TCP [3, 19]. This may explain the observation that the final material loss was enhanced by reducing T/M. The faster degradation rate may be clinically beneficial in that faster degradation would result in higher calcium and phosphate ion release, possibly providing greater potential for bone regeneration [3, 20].

4.4 Effect of filler addition on CHX release

Increase in F% and decrease in T/M (i.e. increase in the MCPM content of each specimen) was found to enhance the water sorption although it did not increase CHX release, possibly because that the absorbed water reacted with β-TCP and MCPM and was 'bound' in resultant brushite crystals. Raising the total filler content did, however, substantially increase drug diffusion. Higher filler addition may create more interfaces between the calcium phosphate particles and the polymer, which could provide the "channel" for small molecules to diffuse out [21]. In addition, increase in the amount of the released drug with progressively increasing filler content may be due to the reduced amount of polymer in the corresponding formulations. The presence of degradable polymer may generate insoluble acidic polymer degradation fragments which could bind basic CHX and thus limit drug release [6]. As shown by factorial analysis, the total filler content was the only significant factor affecting the CHX release rate, indicating that adjustment of the filler/polymer content may be a useful means of controlling CHX release from such adhesives.

4.5 Effect of CHX and filler addition on antibacterial activity

Addition of CHX to the bone adhesives resulted in substantial antibacterial activity, demonstrating that CHX released from the polymer and composites in the first 24 h could effectively inhibit the growth of *S. aureus* (including methicillin-susceptible and resistant strains). Higher filler content was found to generate larger bacterial inhibition zones, indicative of a higher antibacterial activity. The ability to inhibit bacterial growth is often regarded as a critical step in infection prevention, thereby improving the life of orthopedic medical implants [5].

5 Conclusions

The PGLA-DMA based bone adhesives containing CHX have been found to be rapid setting, degradable and with controllable drug release properties, making them potentially suitable as antibacterial bone adhesives. The addition of CHX had no effect on either the material polymerization or subsequent degradation kinetics, although it enhanced initial water sorption and the ratio of resultant brushite to monetite. Increasing the total filler percentage above 50 wt% decreased the adhesive polymerization rate. Early water sorption of the set adhesive discs increased linearly with total MCPM level, while decreasing T/M from 4 to 1 substantially enhanced total mass loss at 10 weeks. Drug release was found to occur by diffusion and was enhanced by raising the total filler percentage and reducing polymer content. Growth inhibition of *S. aureus*, including MRSA, was found to increase at higher total filler content.

Acknowledgments This research work was supported by a Dorothy Hodgkins Postgraduate Award to Xin Zhao and by the Engineering

and Physical Sciences Research Council, UK. This work was supported in part by the WCU Program through the National Research Foundation of Korea (NRF) funded by the Ministry of Education, Science and Technology (No. R31-10069). The authors would like to thank Drs Tom Frenkiel and Geoff Kelly at the Medical Research Council, Biomedical NMR Centre for their help with the NMR studies.

References

1. Ho SM, Young AM. Synthesis, polymerisation and degradation of poly(lactide-*co*-propylene glycol)dimethacrylate adhesives. Eur Polym J. 2006;42:1775–85.
2. Young AM, Ho SM, Abou Neel EA, Ahmed I, Barralet JE, Knowles JC, Nazhat SN. Chemical characterization of a degradable polymeric bone adhesive containing hydrolysable fillers and interpretation of anomalous mechanical properties. Acta Biomater. 2009;5:2072–83.
3. Zhao X, Olsen I, Li HY, Gellynck K, Buxton PG, Knowles JC, Salih V, Young AM. Reactive calcium-phosphate-containing poly(ester-*co*-ether) methacrylate bone adhesives: Chemical, mechanical and biological considerations. Acta Biomater. 2010;6:845–55.
4. Bohner M. Reactivity of calcium phosphate cements. J Mater Chem. 2007;17:3980–6.
5. Mourino V, Boccaccini AR. Bone tissue engineering therapeutics: controlled drug delivery in three-dimensional scaffolds. J R Soc Interface. 2010;7:209–27.
6. Young AM, Ho SM. Drug release from injectable biodegradable polymeric adhesives for bone repair. J Control Release. 2008; 127:162–72.
7. Mandal S, Berendt AR, Peacock SJ. *Staphylococcus aureus* bone and joint infection. J Infect. 2002;44:143–51.
8. Nair SP, Williams RJ, Henderson B. Advances in our understanding of the bone and joint pathology caused by *Staphylococcus aureus* infection. Rheumatology. 2000;39:821–34.
9. Nascimento AP, Tanomaru JMG, Matoba F, Watanabe E, Tanomaru M, Ito IY. Maximum inhibitory dilution of mouthwashes containing chlorhexidine and polyhexamethylene biguanide against salivary *Staphylococcus aureus*. J Appl Oral Sci. 2008; 16:336–9.
10. Harris LG, Mead L, Muller-Oberlander E, Richards RG. Bacteria and cell cytocompatibility studies on coated medical grade titanium surfaces. J Biomed Mater Res A. 2006;78A:50–8.
11. Lee DY, Spangberg LSW, Bok YB, Lee CY, Kum KY. The sustaining effect of three polymers on the release of chlorhexidine from a controlled release drug device for root canal disinfection. Oral Surg Oral Med Oral Pathol Oral Radiol Endod. 2005;100:105–11.
12. Riggs PD, Braden M, Patel M. Chlorhexidine release from room temperature polymerising methacrylate systems. Biomaterials. 2000;21:345–51.
13. Nerurkar MJ, Zentner GM, Rytting JH. Effect of chloride on the release of chlorhexidine salts from methyl-methacrylate—2-hydroxyethyl methacrylate copolymer reservoir devices. J Control Release. 1995;33:357–63.
14. Leung D, Spratt DA, Pratten J, Gulabivala K, Mordan NJ, Young AM. Chlorhexidine-releasing methacrylate dental composite materials. Biomaterials. 2005;26:7145–53.
15. Mehdawi I, Abou Neel EA, Valappil SP, Palmer G, Salih V, Pratten J, Spratt DA, Young AM. Development of remineralizing, antibacterial dental materials. Acta Biomater. 2009;5:2525–39.
16. O'Dell LA, Guerry P, Wong A, Abou Neel EA, Pham TN, Knowles JC, Brown SP, Smith ME. Quantification of crystalline phases and measurement of phosphate chain lengths in a mixed phase sample by P-31 refocused INADEQUATE MAS NMR. Chem Phys Lett. 2008;455:178–83.
17. Andrews JM, BSAC Working PS. BSAC standardized disc susceptibility testing method (version 7). J Antimicrob Chemoth. 2008;62:256–78.
18. Grover LM, Gbureck U, Young AM, Wright AJ, Barralet JE. Temperature dependent setting kinetics and mechanical properties of beta-TCP-pyrophosphoric acid bone cement. J Mater Chem. 2005;15:4955–62.
19. Elliott JC. General chemistry of the calcium orthophosphate. In: Structure and chemistry of the apatites and other calcium orthophosphates (studies in inorganic chemistry). Elsevier; 1994. p. 1–61.
20. Ripamonti U. Osteoinduction in porous hydroxyapatite implanted in heterotopic sites of different animal models. Biomaterials. 1996;17:31–5.
21. Lin M, Wang HT, Meng S, Zhong W, Li ZL, Cai R, Chen Z, Zhou XY, Du QG. Structure and release behavior of PMMA/silica composite drug delivery system. J Pharm Sci. 2007;96: 1518–26.